FORUM ORIGINAL RESEARCH COMMUNICATION

Ero1α Regulates Ca^{2+} Fluxes at the Endoplasmic Reticulum–Mitochondria Interface (MAM)

Tiziana Anelli,[1,2,*] Leda Bergamelli,[1,2,*,†] Eva Margittai,[2,‡] Alessandro Rimessi,[3] Claudio Fagioli,[2] Antonio Malgaroli,[1] Paolo Pinton,[3] Maddalena Ripamonti,[1] Rosario Rizzuto,[3] and Roberto Sitia[1,2]

Abstract

Aims: The endoplasmic reticulum (ER) is involved in many functions, including protein folding, redox homeostasis, and Ca^{2+} storage and signaling. To perform these multiple tasks, the ER is composed of distinct, specialized subregions, amongst which mitochondrial-associated ER membranes (MAM) emerge as key signaling hubs. How these multiple functions are integrated with one another in living cells remains unclear. *Results:* Here we show that Ero1α, a key controller of oxidative folding and ER redox homeostasis, is enriched in MAM and regulates Ca^{2+} fluxes. Downregulation of Ero1α by RNA interference inhibits mitochondrial Ca^{2+} fluxes and modifies the activity of mitochondrial Ca^{2+} uniporters. The overexpression of redox active Ero1α increases passive Ca^{2+} efflux from the ER, lowering [Ca^{2+}]$_{ER}$ and mitochondrial Ca^{2+} fluxes in response to IP3 agonists. *Innovation:* The unexpected observation that Ca^{2+} fluxes are affected by either increasing or decreasing the levels of Ero1α reveals a pivotal role for this oxidase in the early secretory compartment and implies a strict control of its amounts. *Conclusions:* Taken together, our results indicate that the levels, subcellular localization, and activity of Ero1α coordinately regulate Ca^{2+} and redox homeostasis and signaling in the early secretory compartment. *Antioxid. Redox Signal.* 16, 1077–1087.

Introduction

THE ENDOPLASMIC RETICULUM (ER) is a multifunctional organelle involved in protein folding and assembly, disulfide bond formation and Ca^{2+} storage. In the ER, signals originating from the unfolded protein response (UPR) intersect with Ca^{2+}- and redox-dependent events (17, 25). Their integration is fundamental for cell differentiation and death decisions (19). To fulfill its many functions, the ER consists of specialized subregions (38, 44), one of which emerges as a key signaling hub: mitochondria-associated membranes (MAM) guarantee physical association with mitochondria, fundamental for Ca^{2+} signaling and cell survival (13). Enriched in Ca^{2+}-handling proteins, oxidoreductases and chaperones, MAM generate microdomains of high [Ca^{2+}], thus activating the mitochondrial Ca^{2+} uniporters (MCU) (12, 13, 16).

The ER is a potential source of hydrogen peroxide (H$_2$O$_2$). Ero1α and Ero1β flavoproteins sustain oxidative protein folding, transferring electrons from cargo proteins via PDI to molecular oxygen, and yielding H$_2$O$_2$ as a by-product (27). In the ER lumen, H$_2$O$_2$ can drive disulfide bond formation via peroxiredoxin 4 (40, 50), an enzyme abundant in secretory cells (5). Other ER resident enzymes may also generate

Innovation

As knowledge on redox homeostasis in the ER and Ca^{2+} storage and signaling proceeds rapidly, much remains to be understood as to how these key regulatory pathways are integrated with one another to harmonize cell physiology. The results of this work reveal a novel connection between redox control and Ca^{2+} signaling. The levels and localization of Ero1α within the early secretory pathway are shown here to control Ca^{2+} fluxes by modulating ERp44 binding and the ER luminal redox status. The observation that a large fraction of Ero1α localizes in MAM, areas of the ER that establish close contacts with mitochondria, explains the dramatic effects of the oxidase on Ca^{2+} fluxes through the latter organelles.

[1]Università Vita-Salute San Raffaele, Milano, Italy.
[2]Division of Genetics and Cell Biology, San Raffaele Scientific Institute, Milano, Italy.
[3]Department of Experimental and Diagnostic Medicine, Section of General Pathology, Interdisciplinary Center for the Study of Inflammation (ICSI), BioPharmaNet, University of Ferrara, Ferrara, Italy.
*These authors contributed equally to this work.
†*Current affiliation:* Department of Experimental and Diagnostic Medicine, Section of General Pathology, University of Ferrara, Ferrara, Italy.
‡*Current affiliation:* Department of Medical Chemistry, Molecular Biology and Pathobiochemistry, Semmelweis University, Budapest, Hungary.

diffusible oxidants (25) that could act as intracellular messengers and impact redox homeostasis (20, 33).

Several findings highlight the existence of tight connections between the ER luminal redox and Ca^{2+} homeostasis. The Ca^{2+}-ATPase SERCA2b, inositol 1,4,5-trisphosphate receptor type 1 (IP3R1), ryanodine receptors (RyRs), and the Ca^{2+}-sensor stromal interaction molecule 1 (STIM1) are all redox-regulated (18, 23, 39, 41). Furthermore, a circuit involving IP3R1 and Ero1α has been recently implicated in the maladaptive shift during prolonged ER stress (22). Ca^{2+} release via IP3R1 is inhibited by ERp44 (18), a multitask chaperone that prevents secretion of mammalian Ero1α and Ero1β and other substrates of thiol-dependent quality control (1, 2, 10, 11, 30). Therefore, the Ero1α–ERp44 axis could play an important role in regulating Ca^{2+} homeostasis and release.

We show here that Ero1α accumulates where the ER establishes contacts with mitochondria (MAM). The levels of redox-active Ero1α impact Ca^{2+} storage and IP3-dependent fluxes. Ero1α silencing has profound effects on mitochondrial Ca^{2+} uptake, likely modifying the MCU activity. Thus, Ero1α links redox and Ca^{2+} homeostasis and signaling in MAM.

Results

Ero1α is enriched in MAM

Subcellular fractionation of HeLa cells revealed that a large fraction of endogenous Ero1α accumulates in MAM (Fig. 1A), confirming recent results (15). As expected, porin (VDAC1) and cytochrome c were enriched in mitochondria (MP), while ribophorin and Grp94 accumulated mainly in microsomes (Mic). Calnexin and IP3R1 distributed similarly between the microsomal and MAM fractions, while ERp44 was slightly more abundant in MAM. PDI was abundant in both MAM and microsomes (not shown). Immunofluorescence analyses confirmed the presence of both ERp44 and Ero1α at sites of contact with mitochondria, where the two proteins partially co-localize (Fig. 1B and Supplementary Fig.1; Supplementary Data are available online at www.liebertonline.com/ars). As previously described (3) ERp44 was abundant also in the ERGIC area (Fig. 1B). In professional secretory cells, such as myeloma cell lines, a larger fraction of endogenous Ero1α accumulated in the ER (not shown). Upon overexpression, Ero1α is found in virtually all substations of the exocytic
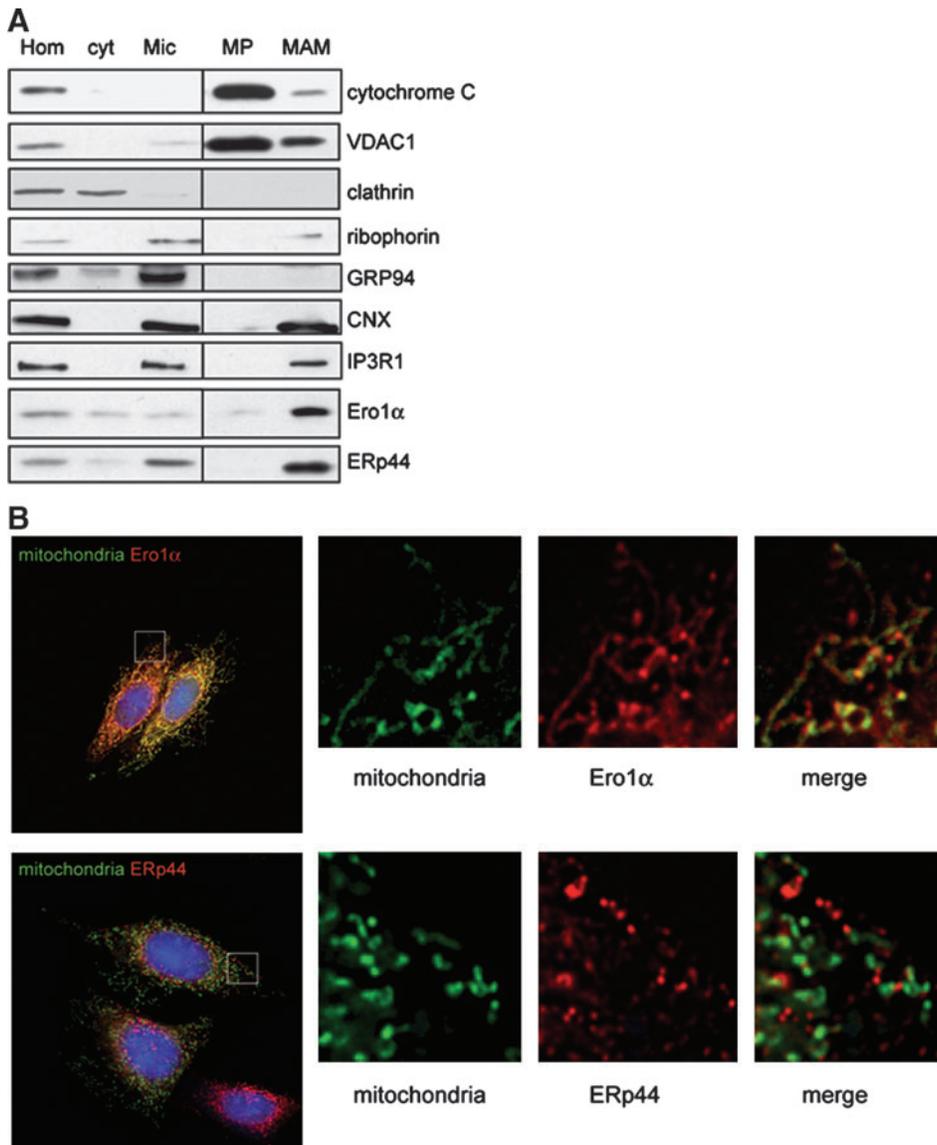

FIG. 1. Ero1α enrichment in MAM. (A) Subcellular fractionation. Aliquots (30 μg protein) from each fraction (48) were resolved under reducing conditions and filters decorated with the indicated antibodies. Cyt, cytosol; Hom, homogenate; Mic, microsomes; MP, mito-pure. Two parts of the same gel, originally separated by irrelevant lanes, are shown. (B) Immunofluorescence. HeLa cells transiently expressing mitochondrial EYFP were stained with anti-Ero1α or anti-ERp44 antibodies as indicated. Ero1α frequently co-localizes with mitochondria, yielding a yellow staining, while ERp44 staining is often adjacent to mitochondria but rarely overlapping. Abundant ERp44 is found in ERGIC and cisGolgi (3). (To see this illustration in color the reader is referred to the web version of this article at www.liebertonline.com/ars).

pathway (not shown) consistent with the notion that Ero1α can saturate the normal localization mechanisms and be secreted (30).

Ero1α levels modulate mitochondrial Ca^{2+} fluxes

In view of the abundance of endogenous Ero1α in MAM, we analyzed its role in Ca^{2+} signaling by silencing or over-expression assays. Ca^{2+} levels and fluxes were monitored by organelle-targeted aequorin probes (31) upon stimulation with histamine, an inositol-1,4,5-trisphosphate (IP3) agonist that activates IP3 receptor (IP3R) channels, causing Ca^{2+} release from ER stores. Ero1α silencing dramatically inhibited mitochondrial Ca^{2+} transients evoked by histamine (Fig. 2A, left panels), while having smaller effects on cytosolic Ca^{2+} (center panels). Blunted Ca^{2+} fluxes were recently

FIG. 2. Ero1α levels modulate Ca^{2+} storage and fluxes. (A) Ero1α silencing. HeLa cells were co-transfected with mitochondrial, cytosolic, or ER aequorin, and Ero1α-specific or control silencing duplexes. Ero1α downregulation drastically lowers mitochondrial Ca^{2+} transients upon histamine stimulation (*left panel,* peak amplitude 61.7±4.2 μM for controls luc2i, $n=36$ vs. 25.1±1.8 μM for Ero1αi, $n=37$, $p<5^*$E-11), having minor effects on cytosolic Ca^{2+} transients (*central panel,* peak amplitude 2.7±0.1 μM for controls luc2i, $n=24$ vs. 2.6±0.1 μM for Ero1αi, $n=24$, $p=0.132$). The steady state [Ca^{2+}]$_{ER}$ is slightly increased in Ero1α siRNA transfectants (*right panel,* plateau values 424.5±22.1 μM, $n=13$ for control; 452.7±22.9 μM, $n=13$ for Ero1αi); $bar=10$ sec. The blot in the *inset,* decorated with anti-Ero1α, shows efficiency of silencing in one representative experiment, PDI providing a loading control. (B) Ero1α over-expression. HeLa cells were co-transfected as in A with wild-type (wt) or mutant Ero1α (C394A), and imaged before or after HIS treatment. Overexpression of Ero1α lowers mitochondrial Ca^{2+} transients (*left panel,* peak amplitude 78.4 μM in controls vs. 55.5 μM for wt Ero1α, $p<0.005$, $n=30$ for both). Only minor effects are observed with the inactive C394A mutant (peak amplitude 72.5 μM, $n=30$). A minor, but still significant effect, is visible in the cyto-

solic Ca^{2+} transients (*central panel,* peak amplitude 2.34±0.06 μM in controls vs. 2.14±0.05 μM for wt E Ero1α, $p<0.05$ and 2.35±0.07 μM for C394A, $n=13$ for all). Moreover, Ero1α overexpression lowers the [Ca^{2+}]$_{ER}$ at steady state, while no significant effects are observed with the C394A mutant (*right panel,* plateau values 477±6 μM, $n=35$ for control; 445±6 μM, $n=32$, $p<0.0005$ for Ero1α; 460±8 μM, $n=37$ for C394A). *Bar*=10 s. The blot shown in the *inset,* decorated with anti-myc antibodies, provides an example of the levels of transfection in one representative experiment; *background bands that serve as loading control.
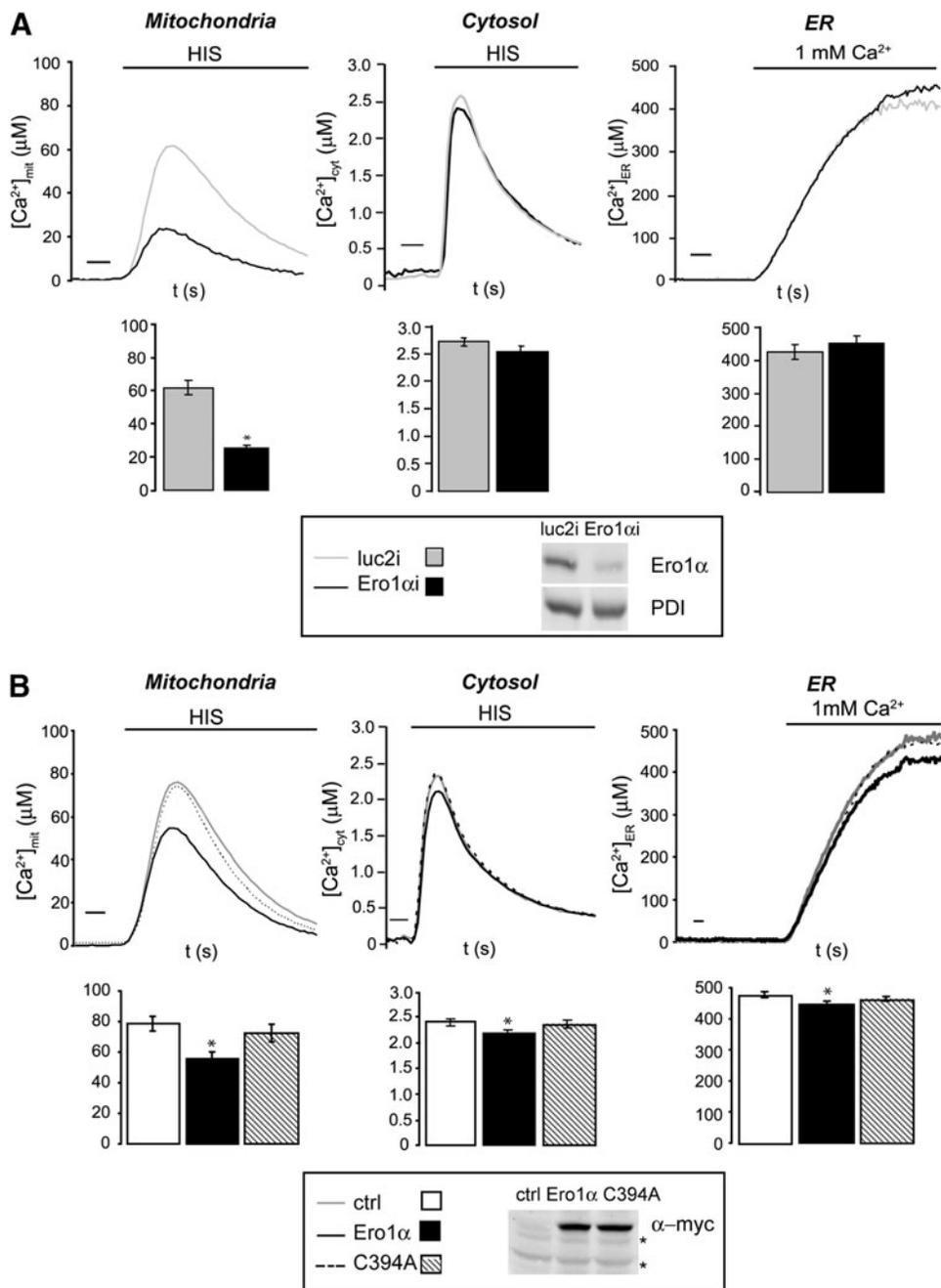
observed also in cardiomyocytes lacking both Ero1α and Ero1β (9). Unexpectedly, also the overexpression of the oxidase inhibited mitochondrial (Fig. 2B left panels) and to a lesser extent cytosolic Ca^{2+} fluxes (center panels). The inactive Ero1α mutant C394A (4, 8) had marginal effects in these assays, excluding that the effects observed were due solely to protein overexpression in the ER and pointing at redox-dependent regulatory mechanism(s).

Hence, either increasing or decreasing Ero1α levels can modify IP3-dependent Ca^{2+} fluxes.

To investigate the underlying mechanisms, we analyzed the concentration of free Ca^{2+} in the ER ([Ca^{2+}]$_{ER}$) by following the refilling of ER stores after ionomycin treatment. As shown in Figure 2B (right panels), cells overexpressing Ero1α displayed significantly lower steady state [Ca^{2+}]$_{ER}$. In contrast, slightly higher [Ca^{2+}]$_{ER}$ were measured upon Ero1α silencing (Fig. 2A, right panels).

[Ca^{2+}]$_{ER}$ is determined by SERCA-dependent Ca^{2+} entry and passive efflux (most likely via IP3R1 (24, 29, 43)). To quantify the former, we analyzed the initial rates of Ca^{2+} ER import, when efflux is negligible (Fig. 3A); Ca^{2+} efflux from the ER in the absence of histamine stimulus was instead measured, after reaching the steady state, by addition of tBuBHQ, a SERCA inhibitor. To minimize artefacts, cells with similar [Ca^{2+}]$_{ER}$ were analyzed in these assays. Ero1α overexpressing cells displayed normal SERCA2b activity but faster passive Ca^{2+} efflux (Fig. 3B). Also in this case, the inactive Ero1α mutant (C394A) had only marginal effects. Thus, active Ero1α facilitates basal ER Ca^{2+} efflux, without affecting the

ER import mechanisms. The net result is a lower [Ca^{2+}]$_{ER}$ in Ero1α overexpressing cells, which translates into less intense efflux peaks in mitochondria and cytosol upon IP3 signaling. A different mechanism must be invoked instead for cells having less Ero1α, that have slightly higher [Ca^{2+}]$_{ER}$. Moreover, no difference in ER Ca^{2+} uptake or Ca^{2+} leakage can be observed upon Ero1α silencing (Figs. 3C and 3D).

Ero1α modulates IP3R1 binding to ERp44

Excess Ero1α binds endogenous ERp44, competing with many endogenous substrates (1, 2, 14, 26, 46). Since ERp44 inhibits IP3R1 (18), the increased Ca^{2+} efflux from the ER in Ero1α transfectants could reflect competition of the oxidase with IP3R1 for ERp44 binding, *de facto* facilitating channel opening (18). Co-immunoprecipitation assays revealed that indeed less IP3R1 associated with ERp44 in Ero1α transfectants, despite similar IP3R1 levels were present in the lysates (Fig. 4). However, also the C394A mutant competed for ERp44 binding. Therefore, since C394A transfectants displayed only marginal changes in [Ca^{2+}]$_{ER}$ or efflux rates (Figs. 2B, 3A, and 3B), the effects of wt Ero1α can only in part depend on competitive ERp44 binding, confirming the involvement of redox-dependent regulatory mechanism(s).

Ero1α levels affect the affinity of the mitocondrial Ca^{2+} uniporter

As shown above, both Ero1α silencing or overexpression impacted mitochondrial Ca^{2+} fluxes. The minor changes in
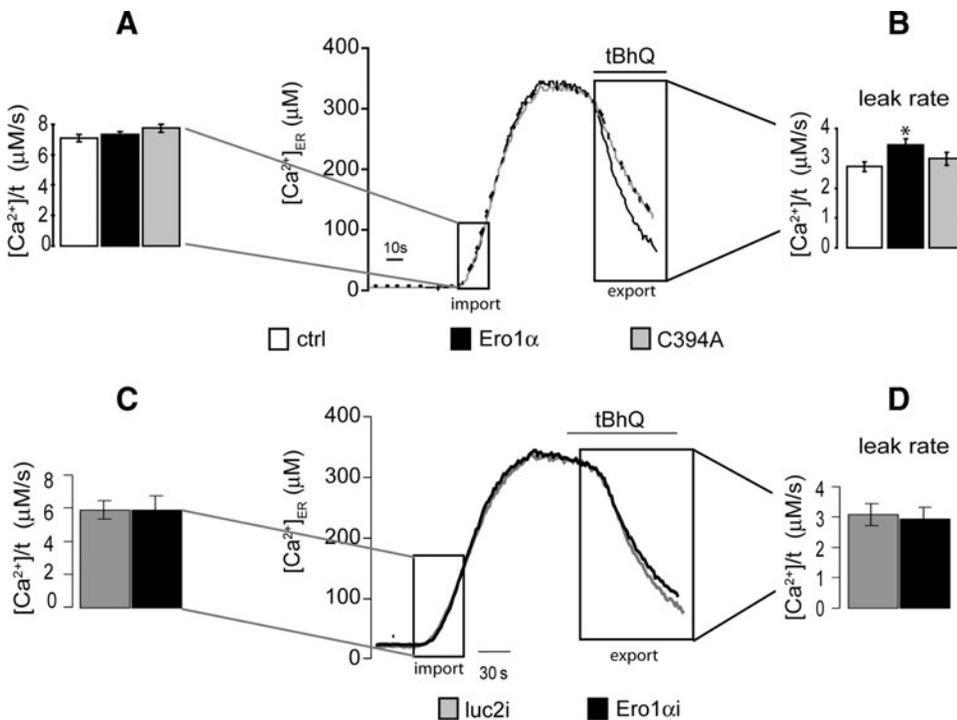

FIG. 3. **Ero1α levels impact Ca^{2+} efflux from the ER.** HeLa cells were transiently transfected with wild-type (wt) or mutant Ero1α (C394A) or empty vector as control **(A, B)**, or subjected to Ero1α silencing (as a control, a treatment with unrelated duplexes was perfomed, Luc2i) **(C, D)**. **(A)** Ero1α overexpression does not modify SERCA2b activity. To measure SERCA activity, the initial phase of the Ca^{2+} uptake curves (examples of which are shown also in Fig. 2) were analyzed and the maximal rate of Ca^{2+} accumulation in the ER calculated. (Maximal rate values: $7.1 \pm 0.3 \,\mu M/s$, $7.3 \pm 0.2 \,\mu M/s$, and $7.7 \pm 0.3 \,\mu M/s$ for controls, Ero1α and C394A, respectively, $n = 30$). **(B)** Ero1α overexpression increases passive Ca^{2+} efflux. Ca^{2+} leak rates were measured by treating cells with the SERCA blocker tBuBHQ soon after a plateau level was reached in the ER. Note that to reduce artefacts, cells with similar plateau levels were compared. ($2.7 \pm 0.2 \,\mu M/s$, $n = 23$, vs. $3.5 \pm 0.2 \,\mu M/s$, $n = 26$, $p < 0.01$ for Ero1α and $2.9 \pm 0.2 \,\mu M/s$, $n = 17$, for C394A, for plateau values between 250–350 μM). *Bar* = 10 s. **(C, D)** Ero1α silencing affects neither SERCA2b activity (Maximal rate values: $5.67 \pm 0.7 \,mM/s$ and $5.77 \pm 0.9 \,mM/s$ for controls and Ero1αi, respectively, $n = 10$), nor passive Ca^{2+} leak from the ER ($3.02 \pm 0.5 \,mM/s$, $n = 10$, vs. $2.93 \pm 0.6 \,mM/s$, $n = 10$ for control and Ero1αi-treated cells with plateau values between 250–350 μM). *Bar* = 30 s.
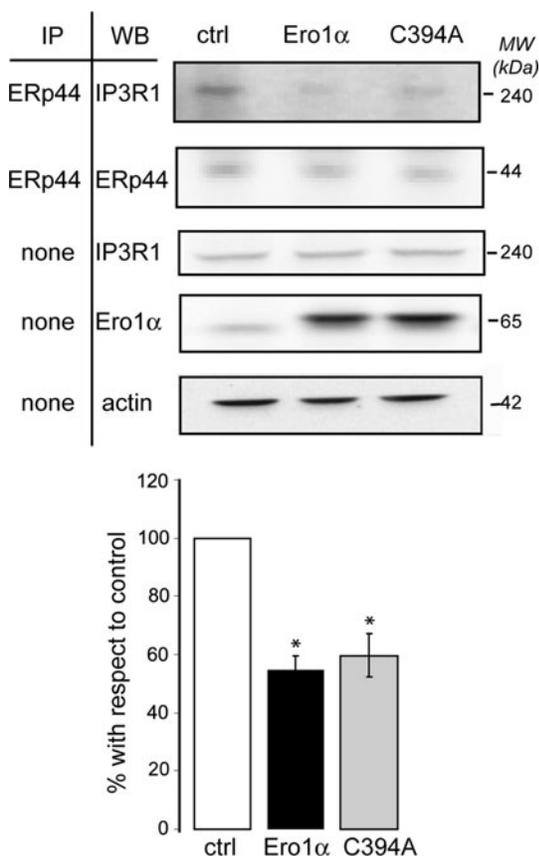
FIG. 4. Ero1α influences IP3R1 binding to ERp44. Aliquots of the lysates or the anti-ERp44 immunoprecipitates (IP) from HeLa cells transfected as indicated were analyzed by WB with the indicated antibodies. Significantly less IP3R1 co-precipitates with ERp44 in HeLa cells overexpressing either wt Ero1α or the mutant C394A, despite similar pools of the two molecules present in the lysates. Densitometric analysis of 3 independent experiments is shown in the bottom panel. *$p < 0.05$ T test.

$[Ca^{2+}]_{ER}$ observed upon Ero1α silencing (Fig. 2A) (22) could hardly explain the dramatic reduction observed on mitochondrial Ca^{2+} fluxes. Rather, its abundance in MAM suggests that endogenous Ero1α regulates Ca^{2+} fluxes locally. We first verified that the integrity of the mitochondrial network and the driving force for Ca^{2+} accumulation were preserved in Ero1α silenced cells (Supplementary Figs. 2A and 2B). We thus hypothesised that Ero1α acts as a sensitizer of MCU. To determine whether this was the case, and in particular if Ero1α silencing decreased MCU affinity, we measured mitochondrial Ca^{2+} uptake in semipermeabilized cells (see Methods). When the perfusion buffer was supplemented with exogenous Ca^{2+}, the rise in $[Ca^{2+}]_{mit}$ was severely compromised in cells with low levels of Ero1α (Figs. 5A and 5B). In contrast, Ero1α overexpression had little if any effect (Fig. 5C). ER reloading upon addition of exogenous Ca^{2+} was not significantly affected in cells expressing lower (Figs. 5D and 5E) or higher (Fig. 5F) Ero1α levels, further confirming that the oxidase does not impact SERCA2b activity.

The effects of Ero1α levels on Ca^{2+} uptake were further analyzed using specific inhibitors of the MCU (Ruthenium

Red) or of Ero1 oxidases (EN460 (6)). As shown in Figure 6, inhibiting Ero1α activity by EN460 had even more drastic effects than RNA silencing in preventing mitochondrial Ca^{2+} uptake. As expected, Ruthenium Red inhibited mitochondrial Ca^{2+} loading in this system, displaying synergic effects with Ero1α inhibitors.

Discussion

Redox modifications of the cytosolic IP3R1 portions are known to regulate its activity (7, 43). Our studies also reveal that the luminal regions of the channel are targets of redox regulation. Indeed, the levels and localization of Ero1α, a key player in the control of ER redox homeostasis (28), impact intracellular Ca^{2+} signaling. The abundance of Ero1α in MAM (Fig. 1) (15) explains why mitochondrial Ca^{2+} fluxes are preferentially affected. Figure 7 summarizes our interpretation of the surprising observation that both overexpression and silencing of the oxidase dramatically inhibit mitochondrial Ca^{2+} transients.

IP3-dependent Ca^{2+} transients, particularly mitochondrial ones, are significantly lower in cells producing excess wild-type Ero1α (Fig. 2B) but not an inactive mutant C394A that can also competitively bind ERp44 (Fig. 4A). This observation implies that ER redox modifications are more important than simple competition for ERp44 binding.
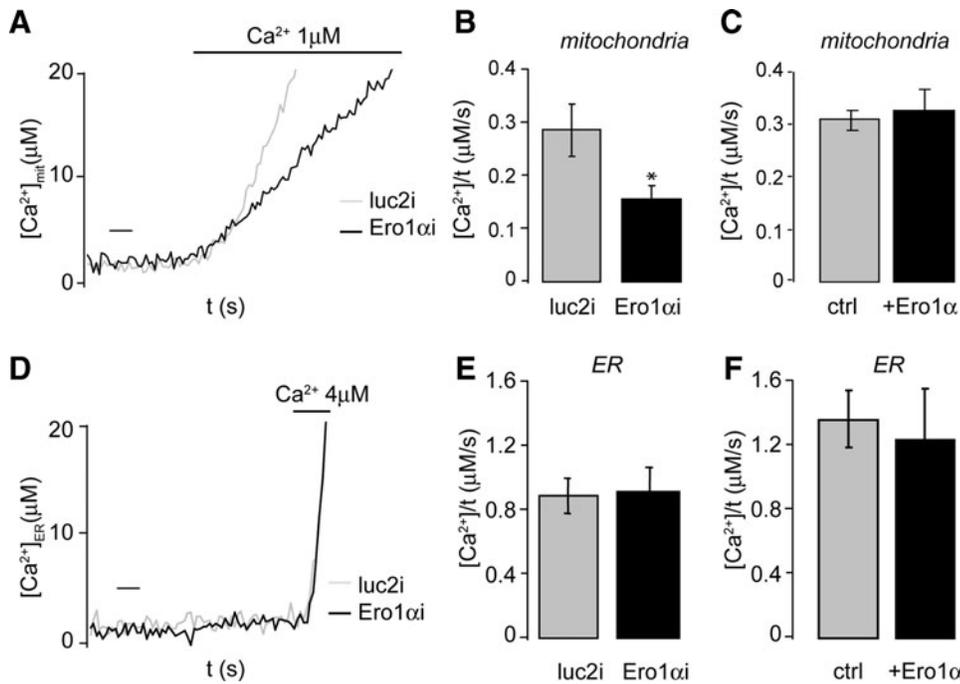
Ero1α levels affected neither the expression levels (not shown) nor the activity of SERCA2b (Figs. 3A–3C, 5D, and 5E), which is instead regulated by the ER-resident oxidoreductase ERp57 (23). These findings underscore the specificity of protein relays in controlling the redox in the ER lumen and confirm that Ero1α has only marginal effects on ERp57 (28). The higher basal efflux from the ER of Ero1α overexpressing cells (Fig. 3B) can explain the lower $[Ca^{2+}]_{ER}$ and in turn the blunted histamine-induced transients observed in Ero1α transfectants.

Conversely, Ero1α downregulation did not affect Ca^{2+} leak from the ER (Fig. 3D), slightly increasing the ER Ca^{2+} store capacity (Fig. 2A), and yet decreased IP3-induced mitochondrial Ca^{2+} transients even more pronouncedly than overexpression (Fig. 2A). The strong effect on mitochondria was not matched by a proportional decrease in cytosolic Ca^{2+} transients. Lower Ero1α levels in MAM seem to slow down the kinetics of IP3R1 oxidation after treatment with DTT (our unpublished results), making it directly or indirectly (via ERp44 or PDI) less responsive to IP3 (18, 42).

Several systems can mediate basal Ca^{2+} efflux from the ER, including IP3R themselves (24, 47). By controlling the re-oxidation kinetics of IP3R1, Ero1α can thus favor Ca^{2+} efflux, though other systems could be involved. The steady state IP3R1 redox state was similar in Ero1α transfectants (data not shown), suggesting that kinetic redox shifts regulate Ca^{2+} exit from the ER.

The observation that in HeLa cells Ero1α accumulates in MAM (Fig. 1A) provides an explanation for the surprisingly similar effects on mitochondrial Ca^{2+} fluxes of down- or up-regulating it (Fig. 7). We hypothesize that in transfected HeLa cells the excess Ero1α acts on IP3R1 channels residing outside MAM, facilitating basal Ca^{2+} efflux. The resulting lower $[Ca^{2+}]_{ER}$ underlies the lower responses to IP3 agonists.

The results shown in Figures 5 and 6 also suggest a specific effect of Ero1α on mitochondrial Ca^{2+} uptake. In the absence

FIG. 5. Silencing Ero1α inhibits mitochondrial Ca^{2+}-uptake. (A–C) HeLa cells, co-transfected with mitochondrial aequorin and Ero1α silencing **(A, B)** or overexpressing **(C)** reagents or controls, were permeabilized with digitonin, and perfused with IB/EGTA. Where indicated, the medium was switched to IB+1 μM Ca^{2+}. Representative traces and average speeds are shown in **A** and **B, C**, respectively (**B**: mean rate values in first 15 s: 0.285 ± 0.05 μM/s, $n=16$ for luc2i controls; 0.155 ± 0.03 μM/s, $n=17$ for Ero1αi; $p=0.018$; **C**: mean rate values: 0.310 ± 0.03 μM/s, n=8 for controls; 0.340 ± 0.030 μM/s, $n=8$ for Ero1α wt); bar=10 s. **(D–F)** Neither Ero1α silencing nor its overexpression significantly affect ER Ca^{2+} uptake. Ca^{2+} uptake into ER was initiated by replacing IB/EGTA with IB+4 μM Ca^{2+}. Representative traces and average speeds are shown, respectively (**E**: mean rate values: 0.88 ± 0.11 μM/s, $n=10$ for luc2i controls; 0.91 ± 0.15 μM/s, $n=10$ for Ero1αi; **F**: mean rate values: 1.38 ± 0.18 μM/s, $n=9$ for controls; 1.24 ± 0.33 μM/s, $n=9$ for Ero1α); bar=10 s.

of detectable alterations in mitochondrial potential or morphology (Supplementary Fig. 2), Ero1α silencing inhibited Ca^{2+} re-uptake by mitochondria in semipermeabilized cells (Figs. 5A and 5B), implying an inter-organellar function for this oxidase. Since we detected no difference in ER uptake under the same conditions, these results argue for a decreased activity of the MCU in Ero1α silenced cells. Accordingly, Ero1α inhibition by pharmacological or genetic means (EN460 or RNAi, respectively) had similar effects on mitochondrial Ca^{2+} uptake, mimicking those obtained with Ruthenium Red, a specific MCU inhibitor (Fig. 6B). In contrast, Ero1α overexpression had little if any effects on mitochondrial import, in accordance with the notion that, when overexpressed, the oxidase accumulates in the ER and other substations of the secretory pathway (30).

Ero1α associates partly with the membrane but does not traverse it (8). Thus, it might exert its activity on mitochondrial Ca^{2+} uptake via associated proteins or by generating diffusible molecules, such as H_2O_2 (37, 45). Contrary to our predictions, Ero1α silencing slightly reduced the association between IP3R1 and ERp44 (EM and RS, data not shown). This unexpected observation suggests that Ero1α (or likely its relative levels) might have further roles in assembling and or maintaining MAM integrity. Ero1α emerges as a good marker for this signaling hub (Fig.1 and (15)), at least in nonprofessional secretory cells. This peculiar distribution explains why its downregulation has more profound effects on mitochondrial than on cytosolic fluxes. As mentioned above, exogenous Ero1α could exert ectopic effects on Ca^{2+} fluxes, possibly regulating IP3R1 localized outside MAM. The insensitivity of mitochondrial uptake in semipermeabilized cells is in line with the observation that overexpressed Ero1α accumulates in the ER and affects the IP3R1 pool localized therein. Recently,

Chop-mediated Ero1α activation was reported to increase IP3R-dependent Ca^{2+} fluxes in ER stressed cells (22). The different outcomes of transfecting Ero1α or inducing it via the Chop pathway could be due to dissimilar subcellular localizations.

The intertwined regulation of Ca^{2+} and redox homeostasis revealed by our experiments might have important pathophysiological implications, particularly during hypoxia and ER stress, when Ca^{2+} tends to leave ER stores towards mitochondria and cytosol. Interestingly, hypoxia relocalizes Ero1α to the ER independently from UPR activation (15). The rate of basal Ca^{2+} efflux from the ER has been reported to regulate mitochondrial metabolism (12). Further studies are needed to dissect how the ER redox status impacts these responses, as these pathways could identify novel therapeutic targets in various diseases where ER stress is involved.

Materials and Methods

Reagents

Mouse monoclonal antibodies anti-ERp44 2D5 (1, 3), anti-Ero1α 2G4 (36) anti-myc 9E10; anti-actin (Sigma Chemical. St. Louis, MO), anti-VDAC1 and rabbit anti-cytochrome c (Calbiochem, Darmstadt, Germany), anti-IP3R1 and anti-ICDH rabbit polyclonal IgG (Abcam); anti-IP3R1 (CT-1, gift from S.K. Joseph, Jefferson University, Philadelphia), anti-clathrin (Cell Signaling, Danvers, MA), anti-calnexin, anti-GRP94, anti-PDI (H-160) rabbit polyclonal IgG, and anti-Grp78 (N-20), goat polyclonal IgG (Santa Cruz Biotechnology, Santa Cruz, CA) and anti-ribophorin (gift from E. Ivessa, Max F Perutz Laboratories, Vienna, Austria) were utilized as described previously or according to the manufacturer's instructions. The Ero1α inhibitor EN460 (6) was kindly provided by David Ron
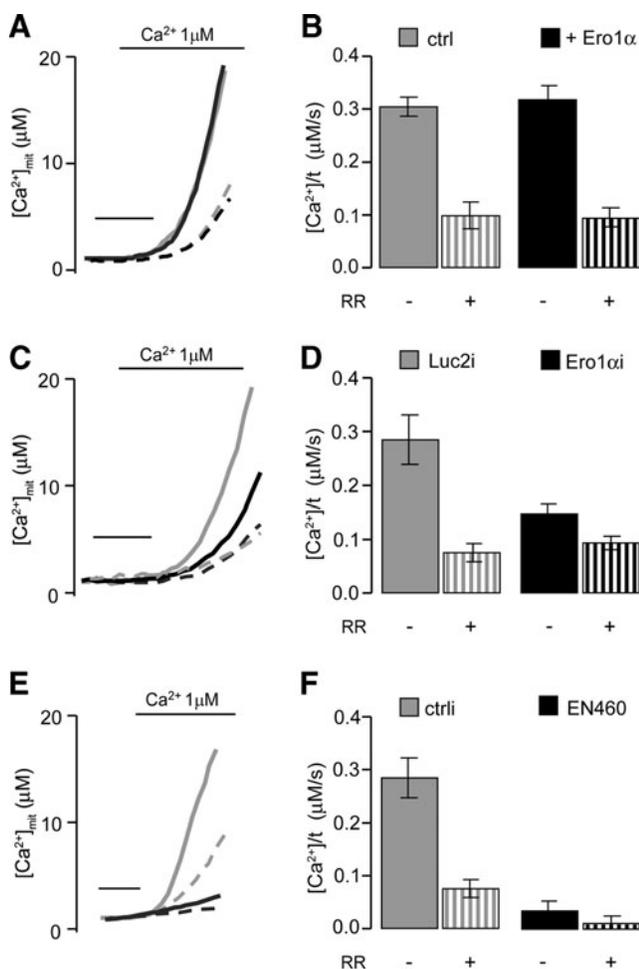
FIG. 6. **Ero1α levels influence the MCU activity.** Effects of Ruthenium Red on mitochondrial Ca²⁺ uptake in Ero1α-overexpressing, Ero1α-silenced, or EN460-treated HeLa cells. HeLa cells, co-transfected with mitochondrial aequorin and Ero1α overexpressing **(A, B)** or silencing **(C, D)** reagents or controls, or treated with the Ero1α inhibitor EN460 **(E, F)** were permeabilized with digitonin and perfused with IB/EGTA. Where indicated, the medium was switched to IB+ 1 μM Ca2+. Representative traces **(A, C, E)** and average speed **(B, D, F)** are shown. RR, Ruthenium Red; *bar*, 10 s. **A and B:** Treatment with Ruthenium Red similarly affects mitochondrial Ca²⁺ uptake in both control and Ero1α overexpressing HeLa cells (**B**: mean rate values in first 15 s: $0.31 \pm 0.02 \, \mu M/s$, $n = 12$ for controls; $0.094 \pm 0.03 \, \mu M/s$, $n = 8$ for controls + RR; $0.34 \pm 0.03 \, \mu M/s$, $n = 12$ for Ero1α; $0.078 \pm 0.02 \, \mu M/s$, $n = 8$ for Ero1α + RR). **C and D:** Inhibition of mitochondrial Ca²⁺ uptake by Ero1α silencing is increased by treatment with Ruthenium Red (**D**: mean rate values in first 15 s: $0.27 \pm 0.05 \, \mu M/s$, $n = 16$ for luc2i controls; $0.066 \pm 0.02 \, \mu M/s$, $n = 12$ for luc2i controls + RR; and $0.14 \pm 0.02 \, \mu M/s$, $n = 16$ for Ero1αi; $0.08 \pm 0.01 \, \mu M/s$, $n = 12$ for Ero1αi + RR). **E and F:** Treatment with the Ero1 inhibitor EN460 drastically impairs mitochondrial Ca²⁺ uptake, mimicking the effects of Ruthenium Red (**F**: mean rate values in first 15 s: $0.283 \pm 0.04 \, \mu M/s$, $n = 14$ for controls; $0.071 \pm 0.02 \, \mu M/s$, $n = 14$ for controls + RR; $0.036 \pm 0.02 \, \mu M/s$, $n = 14$ for EN460 treated cells; $0.005 \pm 0.01 \, \mu M/s$, $n = 14$ for EN460 treated cells + RR).

(Cambridge University, UK); polyclonal anti-ERp44 was from ProteinTech Group, Chicago, IL.

Plasmids encoding myc-tagged human wt Ero1α and its mutant C394A (28), HA-ERp44 (1), cytAEQ, mtAEQ and erAEQ (31) mtGFP (34) mtEYP (Clonthec, Mountain View, CA) were used as described.

Transfection and RNAi

Transfection with aequorin-based (erAEQ, cytAEQ, and mtAEQ) probes was carried out as previously described (35). Ero1α silencing was performed with the following duplexes (36) 5'[CUGUUUUAAGCCACAGACA]3' and 3'[GACAAA AUUCGGUGUCUGU]5'.

Control siRNA (specific for Luciferase2) were obtained from MWG-Biotech AG, Ebersberg Germany. Silencing efficiency of Ero1α, verified by Western blotting (WB), was always ≥70%.

For cytosolic and mitochondrial [Ca²⁺] measurements, transfected cells plated on 13-mm coverslips were incubated with 5 μM coelenterazine for 1–2 h in Krebs-Ringer modified buffer (KRB: 125 mM NaCl, 5 mM KCl, 1 mM Na₃PO₄, 1 mM MgSO₄, 5.5 mM glucose, and 20 mM Hepes, pH 7.4, at 37°C) supplemented with 1 mM CaCl₂, and then transferred to the perfusion chamber. For reconstituting with high efficiency, the AEQ chimeras targeted to the ER (erAEQ), luminal ER [Ca²⁺] was reduced incubating cells for 1 h at 4°C in KRB supplemented with 5 μM coelenterazine, 5 μM ionomycin, and 600 μM EGTA. Cells were then washed with KRB plus 2% BSA and 1 mM EGTA. All AEQ measurements were carried out in KRB, and agonists and other drugs were added to the same medium. Experiments were terminated by lysing cells with 100 μM digitonin in a hypotonic Ca²⁺-rich solution (10 mM CaCl₂ in H₂O), thus discharging the remaining AEQ pool. The light signal was collected and calibrated into [Ca²⁺] values as previously described (31).

To assess mitochondrial Ca²⁺ uptake in permeabilized cells, Ero1α silenced, overexpressing or control cells were transferred to the luminometer chamber and perfused with IB buffer (140 mM KCl, 10 mM NaCl, 1 mM K₃PO₄, 5.5 mM glucose, 2 mM MgSO₄, 1 mM ATP, 2 mM sodium succinate, and 20 mM HEPES, pH 7.05, at 37°C), supplemented with 2 mM EGTA, then permeabilized with 20 μM digitonin for 1 min, and perfused again with IB/EGTA. Ca²⁺ uptake into mitochondria was then initiated by replacing IB/EGTA with IB containing 1 μM Ca²⁺ (IB/Ca²⁺) prepared as described elsewhere (32). To inhibit mitochondrial calcium uniporters, 1 μM Ruthenium Red was added to semipermeabilized cells before and during mitochondrial Ca²⁺ uptake.

To assess ER Ca²⁺ reloading in semipermeabilized cells, luminal ER [Ca²⁺] was reduced incubating cells as described above for the erAEQ probe, and Ca²⁺ uptake was initiated by replacing IB/EGTA with IB containing 4 μM Ca²⁺.

Cell lysis, crosslinking, and immunoprecipitations

Cells were trypsinized, washed in PBS, and incubated for 5 min in ice-cold PBS+ 10 mM NEM, to block disulfide interchange reactions (28). Cells were then lysed in RiPA buffer (150 mM NaCl, 1% NP-40, 0.1% SDS, 10 mM NEM, 5 mM Tris-HCl pH 8.0), plus protease inhibitors. For cross-linking, cells were washed with PBS and incubated with 1 mM Dithiobis succinimidyl propionate (DSP, Pierce, Rockford, IL) for
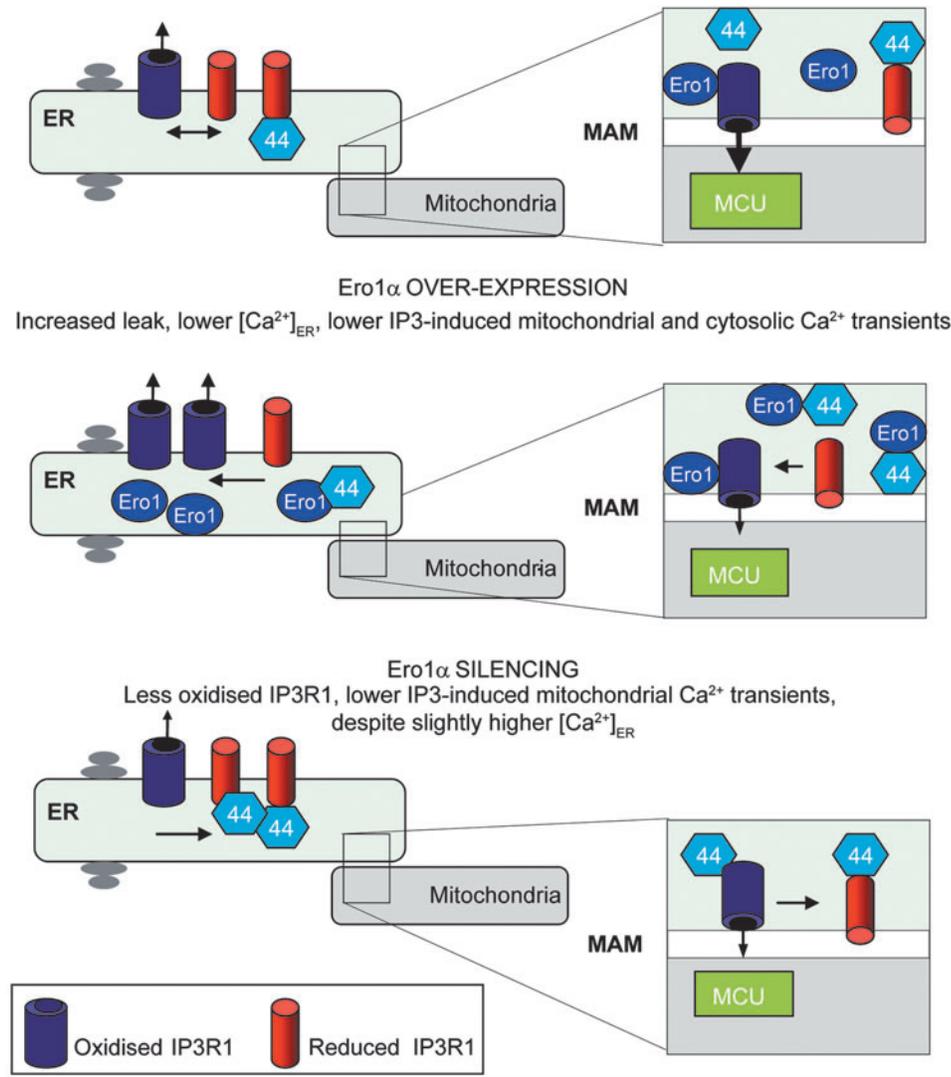
Ero1α OVER-EXPRESSION
Increased leak, lower [Ca²⁺]_ER, lower IP3-induced mitochondrial and cytosolic Ca²⁺ transients

Ero1α SILENCING
Less oxidised IP3R1, lower IP3-induced mitochondrial Ca²⁺ transients, despite slightly higher [Ca²⁺]_ER

Oxidised IP3R1   Reduced IP3R1

FIG. 7. The levels and localization of Ero1α impact Ca²⁺ responses. In physiological conditions (*upper panel*) ERp44 distributes in ERGIC, ER, and MAM, interacting preferentially with reduced IP3R1 and inhibiting the channel activity. At the MAM level, Ero1α can oxidize IP3R1, inhibiting its interactions with ERp44 and thus increasing Ca²⁺ efflux. When overexpressed, most exogenous Ero1α accumulates in the ER (*central panel*). Overexpressed Ero1α may accelerate the rate of IP3R1 oxidation and at the same time decoy ERp44: it can thus increase basal Ca²⁺ efflux from the stores, decrease [Ca²⁺]_ER and consequently inhibit the agonist-induced efflux (and as a consequence mitochondrial responses). With lower Ero1α levels instead (*bottom panel*), also the MAM pool decreases: IP3R1 oxidation is slower, the relative abundance of ERp44 increases, and reduced mitochondrial Ca²⁺ uptake is measured. (To see this illustration in color the reader is referred to the web version of this article at www.liebertonline.com/ars).

30 min at 4°C. The reaction was blocked washing cells twice with PBS+ 20 mM Tris HCl pH 7.4 for 15 min at 4°C. Cells were then lysed as described above directly on the plates. Lysates were pre-cleared with FCS-sepharose beads and incubated with suitable antibodies, previously bound to protein G-sepharose (PGS, Amersham, GE Healthcare Europe) beads. Immunoprecipitated material was resolved under reducing conditions (2%–14% acrylamide gradient SDS-PAGE). WB images were acquired with the Chemidoc-it Imaging System (UVP, Upland, CA) and densitometric analyses performed with Image Quant 5.2.

Measuring SERCA2b activity and ER Ca²⁺ leak

Ca²⁺ uptake rate was analyzed in HeLa transfectants with the Origin50 analysis program considering the first 30 seconds of measurements from the moment of Ca²⁺ addition. For measuring ER Ca²⁺ leak, 36 h after transfection, coverslips were transferred to the luminometer and perfused with KRB/Ca²⁺ until the steady-state [Ca²⁺]_ER was reached. The ER was refilled by exposing cells to extracellular [Ca²⁺] ranging from 0.1 to 1 mM, to obtain different levels of steady state [Ca²⁺]_ER, Since the latter influences the rate of passive efflux, care was taken to select Ero1α-overexpressing or control cells that had

similar [Ca²⁺]_ER plateau values to be compared in the subsequent analysis. Cells were then treated with the SERCA inhibitor tBuBHQ (30 μM) and the consequent decrease of [Ca²⁺]_ER, due to passive efflux, was analyzed. The maximal rates of Ca²⁺ release at different [Ca²⁺]_ER values were calculated for controls and Ero1α transfectants (measured from the first derivative considering 15 sec after tBuBHQ addition). To minimize the effects of the [Ca²⁺]_ER on passive efflux, cells in the 250–350 μM range of plateau values were compared in Figures 3B and 3D.

3D morphological imaging and membrane potential measurement

Cells were transfected with Ero1α-specific or control siRNA duplexes and mt-GFP in a 1:1 ratio. For morphological studies, cells were placed in a thermostatic chamber at 37°C in KRB/Ca²⁺ solution and imaged using an inverted microscope (Axiovert 200M; Carl Zeiss MicroImaging, Inc.) using a 63×/1.4 Plan-Apochromat objective, a Cool-SNAP HQ interline charge-coupled device camera (Roper Scientific) and the MetaMorph 5.0 software (Universal Imaging Corp.). Z-series images were deconvoluted using the PSF-based Exhaustive Photon Reassignment software, running on a

Linux-based PC. For measurement of mitochondrial membrane potential ($\Delta\Psi_m$), cells were loaded with 10 nM tetramethylrhodamine methyl ester (TMRM), and $\Delta\Psi_m$ was measured on a LSM 510 microscope (Carl Zeiss MicroImaging, Inc.) monitoring changes in membrane potential after addition of 10 μM carbonylcyanide p-trifluoromethoxyphenylhydrazone (FCCP), a protonophore that uncouples mitochondrial oxidative phosphorylation. The signal was collected as a total emission > 570 nm.

Immunofluorescence

Cells expressing mtEYFP were fixed with 4% paraformaldehyde and permeabilized with 0.1% TX100. After decoration with antibodies, cells were stained with Hoechst, and analyzed on an Olympus inverted fluorescence microscope (model IX70) with DeltaVision RT Deconvolution System (Alembic, HSR, Milano). After deconvolution, images were processed with Adobe Photoshop 7.0 (Adobe Systems, Inc.). In some experiments, to stain mitochondria cells were treated with 50 nM Mitotracker (Molecular Probes) in Optimem medium for 45 min at 37°C, washed twice with PBS, fixed with methanol, and finally decorated with the indicated antibodies.

Subcellular fractionation

Cells were homogenized and crude mitochondrial and microsomal fractions separated by differential centrifugation. The crude mitochondrial fraction (9000 g pellet) was resuspended in the isolation buffer (250 mM mannitol, 5 mM Hepes, 0.5 mM EGTA, pH 7.4) and further separated on a 30% Percoll gradient (48) to obtain low-density (denoted as MAM) and high-density (denoted as pure mitochondria, Mito Pure) fractions. Aliquots were collected and analyzed by immunoblotting.

Conclusion

Owing to the central signaling role of the ER in physiology and disease, its many functions need to be constantly integrated. Our results demonstrate that endogenous Ero1α, a flavoprotein shown to control oxidative protein folding, accumulates in mitochondrial-associated membranes and modulates Ca^{2+} storage and fluxes. It will be of interst to dissect the mechanisms whereby a luminal oxidase of the ER affects mitochondrial Ca^{2+} uniporters. By coupling redox homeostasis and Ca^{2+} signaling, the Ero1-ERp44 axis can affect "life or death" decisions in many cell types.

Acknowledgments

Author Disclosure Statement

No competing financial interests exist.

References

1. Anelli T, Alessio M, Bachi A, Bergamelli L, Bertoli G, Camerini S, Mezghrani A, Ruffato E, Simmen T, and Sitia R. Thiol-mediated protein retention in the endoplasmic reticulum: the role of ERp44. *EMBO J* 22: 5015–5022, 2003.
2. Anelli T, Alessio M, Mezghrani A, Simmen T, Talamo F, Bachi A, and Sitia R. ERp44, a novel endoplasmic reticulum folding assistant of the thioredoxin family. *EMBO J* 21: 835–844, 2002.
3. Anelli T, Ceppi S, Bergamelli L, Cortini M, Masciarelli S, Valetti C, and Sitia R. Sequential steps and checkpoints in the early exocytic compartment during secretory IgM biogenesis. *EMBO J* 26: 4177–4188, 2007.
4. Bertoli G, Simmen T, Anelli T, Molteni SN, Fesce R, and Sitia R. Two conserved cysteine triads in human Ero1alpha cooperate for efficient disulfide bond formation in the endoplasmic reticulum. *J Biol Chem* 279: 30047–30052, 2004.
5. Bertolotti M, Yim SH, Garcia-Manteiga JM, Masciarelli S, Kim YJ, Kang MH, Iuchi Y, Fujii J, Venè R, Rubartelli A, Rhee SG, and Sitia R. B- to plasma-cell terminal differentiation entails oxidative stress and profound reshaping of the antioxidant responses. *Antioxid Redox Signal* 13: 1133–1144, 2010.
6. Blais JD, Chin KT, Zito E, Zhang Y, Heldman N, Harding HP, Fass D, Thorpe C, and Ron D. A small molecule inhibitor of endoplasmic reticulum oxidation 1 (ERO1) with selectively reversible thiol reactivity. *J Biol Chem* 285:20993–1003, 2010.
7. Bootman MD, Taylor CW, and Berridge MJ. The thiol reagent, thimerosal, evokes Ca2+ spikes in HeLa cells by sensitizing the inositol 1,4,5-trisphosphate receptor. *J Biol Chem* 267: 25113–25119, 1992.
8. Cabibbo A, Pagani M, Fabbri M, Rocchi M, Farmery MR, Bulleid NJ, and Sitia R. ERO1-L, a human protein that favors disulfide bond formation in the endoplasmic reticulum. *J Biol Chem* 275: 4827–4833, 2000.
9. Chin T, Kang G, Qu J, Gardner LB, Coetzee WA, Zito E, Fishman GI, and Ron D. The sarcoplasmic reticulum luminal thiol oxidase ERO1 regulates cardiomyocyte excitation-coupled calcium release and response to hemodynamic load. *FASEB J* 25: 2583–2591, 2011.
10. Cortini M and Sitia R. ERp44 and ERGIC-53 synergize in coupling efficiency and fidelity of IgM polymerization and secretion. *Traffic* 11: 651–659, 2010.
11. Cortini M and Sitia R. From antibodies to adiponectin: Role of ERp44 in sizing and timing protein secretion. *Diabetes Obes Metab* 12: 39–47, 2010.
12. Csordas G, Varnai P, Golenar T, Roy S, Purkins G, Schneider TG, Balla T, and Hajnoczky G. Imaging interorganelle contacts and local calcium dynamics at the ER-mitochondrial interface. *Mol Cell* 39: 121–132. 2010.
13. de Brito OM and Scorrano L. An intimate liaison: Spatial organization of the endoplasmic reticulum-mitochondria relationship. *EMBO J* 29: 2715–2723, 2010.
14. Fraldi A, Zito E, Annunziata F, Lombardi A, Cozzolino M, Monti M, Spampanato C, Ballabio A, Pucci P, Sitia R, and Cosma MP. Multistep, sequential control of the trafficking and function of the multiple sulfatase deficiency gene product, SUMF1 by PDI, ERGIC-53 and ERp44. *Hum Mol Genet* 17: 2610–2621, 2008.

15. Gilady SY, Bui M, Lynes EM, Benson MD, Watts R, Vance JE, and Simmen T. Ero1alpha requires oxidizing and normoxic conditions to localize to the mitochondria-associated membrane (MAM). *Cell Stress Chaperones* 15: 619–629, 2010.

16. Giorgi C, De Stefani D, Bononi A, Rizzuto R, and Pinton P. Structural and functional link between the mitochondrial network and the endoplasmic reticulum. *Int J Biochem Cell Biol* 41: 1817–1827, 2009.

17. Gorlach A, Klappa P, and Kietzmann T. The endoplasmic reticulum: Folding, calcium homeostasis, signaling, and redox control. *Antioxid Redox Signal* 8: 1391–1418, 2006.

18. Higo T, Hattori M, Nakamura T, Natsume T, Michikawa T, and Mikoshiba K. Subtype-specific and ER lumenal environment-dependent regulation of inositol 1,4,5-trisphosphate receptor type 1 by ERp44. *Cell* 120: 85–98, 2005.

19. Hotamisligil GS. Endoplasmic reticulum stress and the inflammatory basis of metabolic disease. *Cell* 140: 900–917, 2010.

20. Janssen-Heininger YM, Mossman BT, Heintz NH, Forman HJ, Kalyanaraman B, Finkel T, Stamler JS, Rhee SG, and van der Vliet A. Redox-based regulation of signal transduction: Principles, pitfalls, and promises. *Free Radic Biol Med* 45: 1–17, 2008.

21. Kang S, Kang J, Kwon H, Frueh D, Yoo SH, Wagner G, and Park S. Effects of redox potential and Ca2+ on the inositol 1,4,5-trisphosphate receptor L3-1 loop region: Implications for receptor regulation. *J Biol Chem* 283: 25567–25575, 2008.

22. Li G, Mongillo M, Chin KT, Harding H, Ron D, Marks AR, and Tabas I. Role of ERO1-alpha-mediated stimulation of inositol 1,4,5-triphosphate receptor activity in endoplasmic reticulum stress-induced apoptosis. *J Cell Biol* 186: 783–792, 2009.

23. Li Y and Camacho P. Ca2+-dependent redox modulation of SERCA 2b by ERp57. *J Cell Biol* 164: 35–46, 2004.

24. Lomax RB, Camello C, Van Coppenolle F, Petersen OH, and Tepikin AV. Basal and physiological Ca(2+) leak from the endoplasmic reticulum of pancreatic acinar cells. Second messenger-activated channels and translocons. *J Biol Chem* 277: 26479–26485, 2002.

25. Margittai E and Sitia R. Oxidative protein folding in the secretory pathway and redox signaling across compartments and cells. *Traffic* 12: 1–8, 2011.

26. Mariappan M, Radhakrishnan K, Dierks T, Schmidt B, and von Figura K. ERp44 mediates a thiol-independent retention of formylglycine-generating enzyme in the endoplasmic reticulum. *J Biol Chem* 283: 6375–6383, 2008.

27. Masciarelli S and Sitia R. Building and operating an antibody factory: Redox control during B to plasma cell terminal differentiation. *Biochim Biophys Acta* 1783: 578–588, 2008.

28. Mezghrani A, Fassio A, Benham A, Simmen T, Braakman I, and Sitia R. Manipulation of oxidative protein folding and PDI redox state in mammalian cells. *EMBO J* 20: 6288–6296, 2001.

29. Oakes SA, Scorrano L, Opferman JT, Bassik MC, Nishino M, Pozzan T, and Korsmeyer SJ. Proapoptotic BAX and BAK regulate the type 1 inositol trisphosphate receptor and calcium leak from the endoplasmic reticulum. *Proc Natl Acad Sci USA* 102: 105–110, 2005.

30. Otsu M, Bertoli G, Fagioli C, Guerini-Rocco E, Nerini-Molteni S, Ruffato E, and Sitia R. Dynamic retention of Ero1alpha and Ero1beta in the endoplasmic reticulum by interactions with PDI and ERp44. *Antioxid Redox Signal* 8: 274–282, 2006.

31. Pinton P, Rimessi A, Romagnoli A, Prandini A, and Rizzuto R. Biosensors for the detection of calcium and pH. *Methods Cell Biol* 80: 297–325, 2007.

32. Rapizzi E, Pinton P, Szabadkai G, Wieckowski MR, Vandecasteele G, Baird G, Tuft RA, Fogarty KE, and Rizzuto R. Recombinant expression of the voltage-dependent anion channel enhances the transfer of Ca2+ microdomains to mitochondria. *J Cell Biol* 159: 613–624, 2002.

33. Rhee SG, Kang SW, Jeong W, Chang TS, Yang KS, and Woo HA. Intracellular messenger function of hydrogen peroxide and its regulation by peroxiredoxins. *Curr Opin Cell Biol* 17: 183–189, 2005.

34. Rizzuto R, Brini M, De Giorgi F, Rossi R, Heim R, Tsien RY, and Pozzan T. Double labelling of subcellular structures with organelle-targeted GFP mutants in vivo. *Curr Biol* 6: 183–188, 1996.

35. Rizzuto R, Pinton P, Carrington W, Fay FS, Fogarty KE, Lifshitz LM, Tuft RA, and Pozzan T. Close contacts with the endoplasmic reticulum as determinants of mitochondrial Ca^{2+} responses. *Science* 280: 1763–1766, 1998.

36. Ronzoni R, Anelli T, Brunati M, Cortini M, Fagioli C, and Sitia R. Pathogenesis of ER storage disorders: Modulating Russell body biogenesis by altering proximal and distal quality control. *Traffic* 11: 947–957, 2010.

37. Sevier CS, Qu H, Heldman N, Gross E, Fass D, and Kaiser CA. Modulation of cellular disulfide-bond formation and the ER redox environment by feedback regulation of Ero1. *Cell* 129: 333–344, 2007.

38. Sitia R and Meldolesi J. Endoplasmic reticulum: A dynamic patchwork of specialized subregions. *Mol Biol Cell* 3: 1067–1072, 1992.

39. Sun J, Xin C, Eu JP, Stamler JS, and Meissner G. Cysteine-3635 is responsible for skeletal muscle ryanodine receptor modulation by NO. *Proc Natl Acad Sci USA* 98: 11158–11162, 2001.

40. Tavender TJ and Bulleid NJ. Peroxiredoxin IV protects cells from oxidative stress by removing H_2O_2 produced during disulphide formation. *J Cell Sci* 123: 2672–2679, 2010.

41. Trebak M, Ginnan R, Singer HA, and Jourd'heuil D. Interplay between calcium and reactive oxygen/nitrogen species: An essential paradigm for vascular smooth muscle signaling. *Antioxid Redox Signal* 12: 657–674, 2010.

42. Valetti C and Sitia R. The differential effects of dithiothreitol and 2-mercaptoethanol on the secretion of partially and completely assembled immunoglobulins suggest that thiol-mediated retention does not take place in or beyond the Golgi. *Mol Biol Cell* 5: 1311–1324, 1994.

43. Vanlingen S, Sipma H, De Smet P, Callewaert G, Missiaen L, De Smedt H, and Parys JB. Modulation of inositol 1,4,5-trisphosphate binding to the various inositol 1,4,5-trisphosphate receptor isoforms by thimerosal and cyclic ADP-ribose. *Biochem Pharmacol* 61: 803–809, 2001.

44. Voeltz GK, Rolls MM, and Rapoport TA. Structural organization of the endoplasmic reticulum. *EMBO Rep* 3: 944–950, 2002.

45. Wang L, Li SJ, Sidhu A, Zhu L, Liang Y, Freedman RB, and Wang CC. Reconstitution of human Ero1-Lalpha/protein-disulfide isomerase oxidative folding pathway in vitro. Position-dependent differences in role between the a and a' domains of protein-disulfide isomerase. *J Biol Chem* 284: 199–206, 2009.

46. Wang ZV, Schraw TD, Kim JY, Khan T, Rajala MW, Follenzi A, and Scherer PE. Secretion of the adipocyte-specific secretory protein adiponectin critically depends on thiol-mediated protein retention. *Mol Cell Biol* 27: 3716–3731, 2007.

47. White C, Li C, Yang J, Petrenko NB, Madesh M, Thompson CB, and Foskett JK. The endoplasmic reticulum gateway to

apoptosis by Bcl-X(L) modulation of the InsP3R. *Nat Cell Biol* 7: 1021–1028, 2005.

48. Wieckowski MR, Giorgi C, Lebiedzinska M, Duszynski J, and Pinton P. Isolation of mitochondria-associated membranes and mitochondria from animal tissues and cells. *Nat Protoc* 4: 1582–1590, 2009.

49. Yoshikawa F, Iwasaki H, Michikawa T, Furuichi T, and Mikoshiba K. Trypsinized cerebellar inositol 1,4,5-trisphosphate receptor. Structural and functional coupling of cleaved ligand binding and channel domains. *J Biol Chem* 274: 316–327, 1999.

50. Zito E, Melo EP, Yang Y, Wahlander Å, Neubert TA, and Ron D. Oxidative protein folding by an endoplasmic reticulum-localized peroxiredoxin. *Mol Cell* 40: 787–797, 2010.

Address correspondence to;
Dr. Roberto Sitia
San Raffaele Scientific Institute
Vita-Salute University
Via Olgettina 58
Milan 20132
Italy

E-mail: r.sitia@hsr.it

Abbreviations Used

CNX = calnexin
cytAEQ = cytosolic aequorin
ER = endoplasmic reticulum
erAEQ = ER aequorin
Ero1 = endoplasmic reticulum oxidoreductin 1
ERp44 = endoplasmic reticulum protein 44kDa
GRp94 = glucose regulated protein 94kDa
IP3R1 = inositol 1,4,5-trisphosphate receptor type 1
MAM = mitochondria-associated membranes
MCU = mitochondrial Ca²⁺ uniporters
mtAEQ = mitochondrial aequorin
QC = quality control
SERCA = sarcoendoplasmic reticulum Ca²⁺ ATPase
tBuBHQ = 2,5-di-(tertbutyl)-1,4-benzohydroquinone
VDAC = voltage-dependent anion channel